ORGANOMETALLICS

Article

Cite This: *Organometallics* XXXX, XXX, XXX−XXX

pubs.acs.org/Organometallics

Pt−M (M = Au and Tl) Dative Bonds Using Bis(cyclometalated)platinum(II) Complexes

Sheida Rajabi,[†] Sirous Jamali,*[,†] Soroosh Naseri,[†] Ali Jamjah,[†] Reza Kia,[†] Hamidreza Samouei,[‡] Piero Mastrorilli,[§] Hamid R. Shahsavari,[∥] and Paul R. Raithby[⊥]

[†]Chemistry Department, Sharif University of Technology, P.O. Box 11155-3516, Tehran 1458889694, Iran

[‡]Department of Chemistry, Texas A&M University, P.O. Box 30012, College Station, Texas 77842-3012, United States

[§]DICATECh, Politecnico di Bari, Bari I-70125, Italy

[∥]Department of Chemistry, Institute for Advanced Studies in Basic Sciences (IASBS), Zanjan 45137-66731, Iran

[⊥]Department of Chemistry, University of Bath, Claverton Down, Bath BA2 7AY, U.K.

Supporting Information

ABSTRACT: Symmetrical and unsymmetrical biscyclometalated platinum(II) complexes $[Pt(ptpy)_2]$, **1**, and [Pt(ptpy)(bppy)], **2**, in which ptpy = deprotonated 2-(*p*-tolyl)pyridine and bppy = deprotonated 2-(3-bromophenyl)pyridine, have been prepared from the reaction between tris(pentafluorophenyl)borane, $B(C_6F_5)_3$ and 1 equiv of monocyclometalated complexes [PtMe(ptpy)(ptpyH)], **B**, and [PtMe(ptpy)(bppyH)], **C**, respectively. The solid-state structures of **1** and **2** have been determined by X-ray crystallography. The reaction of **1** with 1 equiv of $TlPF_6$ or $[Au(PPh_3)]OTF$ resulted in the production of heteronuclear complexes $[Pt(ptpy)_2Tl]PF_6$, **3** and $\{Pt(ptpy)_2[Au(PPh_3)]\}OTF$, **4**, respectively. X-ray diffraction data showed that in solid state, complex **4** exists as a mixture of supported and unsupported Pt^{II}−Au^{I}-bonded structures, whereas complex **3** consists of an infinite helical chain structure built up by unsupported Pt−Tl dative bonds. Absorption, emission, and NMR spectroscopy data showed that both Pt−Tl and Pt−Au bonds in **3** and **4** have dynamic behavior. The low-temperature ^1H, $^{31}P\{^1H\}$, and exchange spectroscopy NMR of **4** revealed two dynamic behaviors involving the rupture of the Au−C_{ipso} bond as well as the dissociation−association of the $[Au(PPh_3)]^+$ and $Pt(ptpy)_2$ fragments. All complexes displayed bright emission in the solid state, and their absorption and emission properties have been investigated both experimentally and by time-dependent density functional theory calculations.

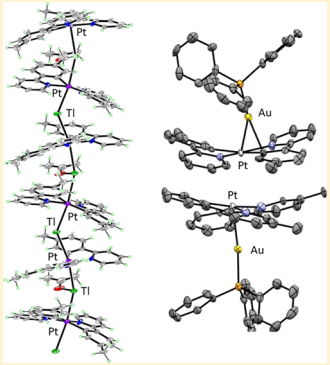

INTRODUCTION

Metal−metal bonding interactions have been employed as important tools for the synthesis of multinuclear complexes, extended structures, and self-assembled systems and provide opportunities for tuning the chemical and physical properties of these compounds.[1] Transmetalation is an important reaction step in palladium catalyzed C−C bond coupling reactions. It has been shown that these reactions proceed through intermediates containing a $M(d^8)$−$M'(d^{10})$ bond.[2] Very recently, bis(cyclometalated)palladium(II) complexes containing Pd^{II}−Zn^{II} and Pd^{II}−Cu^{I} have been prepared and their solid-state structures have been determined using X-ray crystallography.[3] In addition, cyclometalated platinum(II)−gold(I) and platinum(II)−silver(I) complexes have been recently described displaying unusual Pt−Au and Pt−Ag bonds that are supported by Au−C_{ipso} and Ag−C_{ipso} bonds, respectively, and are considered as snapshots of transmetalation of an aryl group between the platinum and gold or silver centers.[4] On the other hand, d^8−d^{10} and d^8−s^2 metal−metal interactions play a key role in the synthesis as well as in the emission properties of metal−metal bonded chains and entities. For example, helical chains $\{[Pt(\hat{C}N)_2]_2[Ag(acetone)]_2\}_n$ $(ClO_4)_{2n}$·*n*-acetone, in which $\hat{C}N$ = deprotonated 2-phenylpyridine or 2-(2-thienyl)pyridine, have been built up by Pt−Ag dative bonds formed from the reaction between the corresponding cyclometalated platinum complex $Pt(\hat{C}N)_2$ and $AgClO_4$.[5] It has also been demonstrated that platinum(II) complexes containing C_6F_5 or alkynyl ligands and thallium(I) salts can form linear or helical chains $[-Pt^{II}-Tl^{I}-]_\infty$ via Pt−Tl dative bonds. These entities and extended chains display interesting optical properties such as mechanochromic, solvochromic, and thermochromic luminescence behaviors.[6] We have recently reported a tetranuclear linear Pt_2Tl_2 chain that is formed by Pt^0−Tl^{I} dative bonds and a strong Tl^{I}−Tl^{I} closed-shell interaction, indicating an intense red emission originated from a platinum to thallium−thallium charge-transfer excited state.[7] However, these metal−metal bonding interactions are rather weak and undergo a dynamic cleavage and recombination in solution. The dynamic nature of these noncovalent interactions plays an important role in many research areas such as supramolecular self-assembly, molecular

Received: December 15, 2018

DOI: 10.1021/acs.organomet.8b00907
Organometallics XXXX, XXX, XXX−XXX

switching, optoelectronic materials, and transmetalation reactions.[4,8] In this area, a great number of complexes containing dynamic Pt−M (M = Tl) bonding interactions have been investigated.[6,9] Recently, it has been shown that the cationic phosphide-bridged complexes of the type $[\{M'PtM(\mu\text{-}PPh_2)_2(C_6F_5)_2(PPh_3)_2\}]^+$, in which M = Pd or Pt and M′ = Ag or Au, display a dynamic behavior of the coordinated fragment $M'(PPh_3)$ (Scheme 1). $^{31}P\{^1H\}$ exchange spectroscopy

Scheme 1

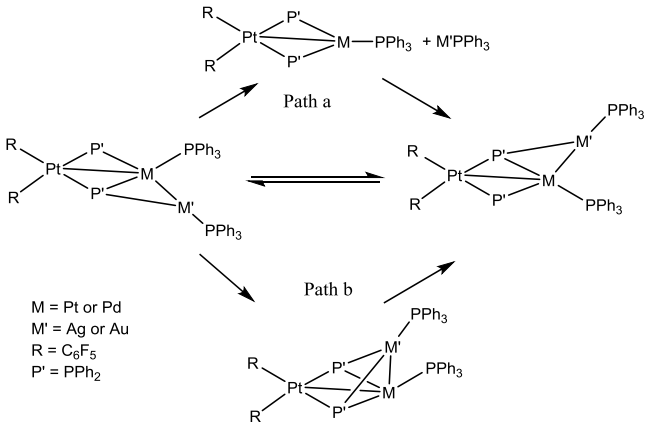

(EXSY) showed that the dynamic process for M′ = Ag involves a dissociation−association (Scheme 1, path a) of the two fragments $(C_6F_5)_2Pt(\mu\text{-}PPh_2)_2M(PPh_3)$ and $[Ag(PPh_3)]^+$, while for M′ = Au, it involves an intramolecular rearrangement (Scheme 1, path b) of the $[Au(PPh_3)]^+$ fragment.[10]

These NMR data showed a lability of the $[Au(PPh_3)]^+$ lower than those of $[Ag(PPh_3)]^+$. Dynamic processes involving $[Ag(PPh_3)]^+$ adducts of anionic or neutral phosphido bridged diplatinum complexes have been also described.[11] The lower lability of the $[Au(PR_3)]^+$ fragment in comparison to $[Ag(PR_3)]^+$ has been also shown in bis-cyclometalated platinum(II) complexes of type $[PtL'(bdt)\{Au(PCy_3)\}]$, in which L′ = 2-phenylpyridine or 1-(4-tertbutylphenyl)-isoquinoline, bdt = 1,2-benzenedithiolate. Similarly, in the cyclometalated complex $[(CNC)(PPh_3)PtAu(PPh_3)](ClO_4)$, in which CNC = 2,6-diphenylpyridine, a lower lability for the $[Au(PPh_3)]^+$ fragments is observed. This complex underwent intramolecular rearrangement dynamic processes involving the migration of the $[Au(PR_3)]^+$ units between the S atoms or C_{ipso} atoms of the dithiolate or 2,6-diphenylpyridine ligands, respectively.[4,12] Pursuing our studies on the synthesis of cyclometalated platinum complexes and on homo- and heteronuclear metal−metal bonding interactions in these systems,[7,13] in this study, we report a new synthetic method for the preparation of symmetrical and unsymmetrical bis(cyclometalated)platinum(II) complexes $[Pt(ptpy)_2]$, **1**, and $[Pt(ptpy)(bppy)]$, **2**, respectively, in which ptpy = deprotonated 2-(*p*-tolyl)pyridine and bppy = deprotonated 2-(3-bromophenyl)pyridine. This type of bis-cyclometalated complex which reveals interesting emission features has been used as a triplet emitter dopant in organic light-emitting diodes and has served as a case study for the characterization of the triplet substates.[14] The metal−metal interactions in these complexes can be utilized to generate interesting multinuclear complexes or extended chains and to change optical properties of the parent complexes. In the following, we have examined the reactions of **1** with $TlPF_6$ and $[Au(PPh_3)]^+$ that yielded to the extended helical chain $[-Pt^{II}-Tl^{I}-]_\infty$, **3**, and the binuclear $Pt^{II}-Au^{I}$ complex, **4**, respectively.

RESULT AND DISCUSSION

Synthesis and Characterization. von Zelewsky et al. have reported the synthesis of bis(cyclometalated)platinum complexes from lithiated ligands and $PtCl_2(SEt_2)_2$.[15] In their proposed method, the lithiated ligands must be prepared from the corresponding halides which are usually synthesized as a mixture of regioisomeric products and require difficult techniques for their separation and purification.[16] Very recently, González-Herrero and co-workers reported a facile approach for synthesizing homoleptic and heteroleptic bis-(cyclometalated) platinum(II) complexes by photochemical C−H bond activation in methylplatinum(II) complexes.[17] However, it should be note that the crystal structure of the above-mentioned complexes had not been determined. Besides, one cannot expect to obtain good quality single crystals when the complexes are prepared based on the previously mentioned photochemical method. As shown in Scheme 2, the reaction of the dimeric platinum(II) complex $[Pt_2Me_4(\mu\text{-}SMe_2)_2]$ with 2 equiv of ptpyH ligand yields the cyclometalated platinum(II) complex of type $[PtMe(SMe_2)(ptpy)]$, **A**. Complex **A** has a labile dimethyl sulfide ligand that can be replaced by N atom of a similar (ptpyH) or of a different (bppyH) cyclometalating ligand leading to methylplatinum(II) complexes $[PtMe(ptpy)(ptpyH)]$, **B**, and $[PtMe(ptpy)(bppyH)]$, **C**, respectively. Removing the free dimethylsulfide by purging the solution with Ar for several hours, followed by the addition of tris(pentafluorophenyl)borane, leads to the production of bis(cyclometalated)platinum(II) complexes **1** and **2** in good yields. The C−H bond activation by platinum(II) complexes in the presence of $B(C_6F_5)_3$ is a well-known process and has been reported by several research groups over the past 2 decades.[18] Bis-cyclometalated

Scheme 2

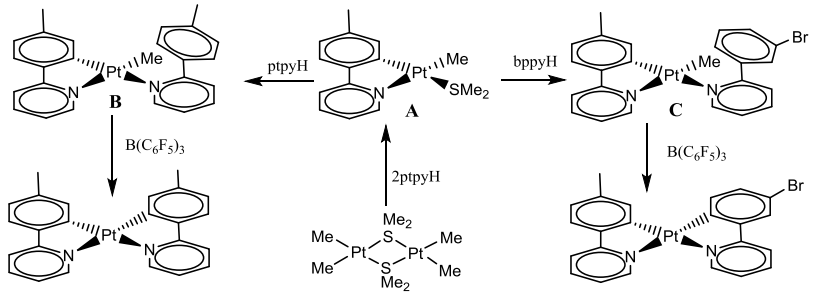

DOI: 10.1021/acs.organomet.8b00907
Organometallics XXXX, XXX, XXX−XXX

complexes **1** and **2** were stable in acetone solution for several days and were characterized using NMR spectroscopy in solution and by X-ray crystallography in solid state. The NMR spectra of **1** were the same as that reported previously (Figures S1–S3).[17] The NMR spectra [^{1}H, ^{13}C and (^{1}H,^{1}H)-COSY-DQ] of the new complex **2** confirmed the structure of the complex in solution (Figures S4–S6″).

Crystals of **1** and **2** suitable for X-ray crystallography were obtained by slow vapor diffusion of *n*-hexane into acetone solutions of **1** and **2**, respectively. These complexes crystallized in the monoclinic system, with space group $P2_1/n$. The molecular crystal structures and crystal data of **1** and **2** are shown in Figure 1a,b and Tables S1–S6, respectively. The

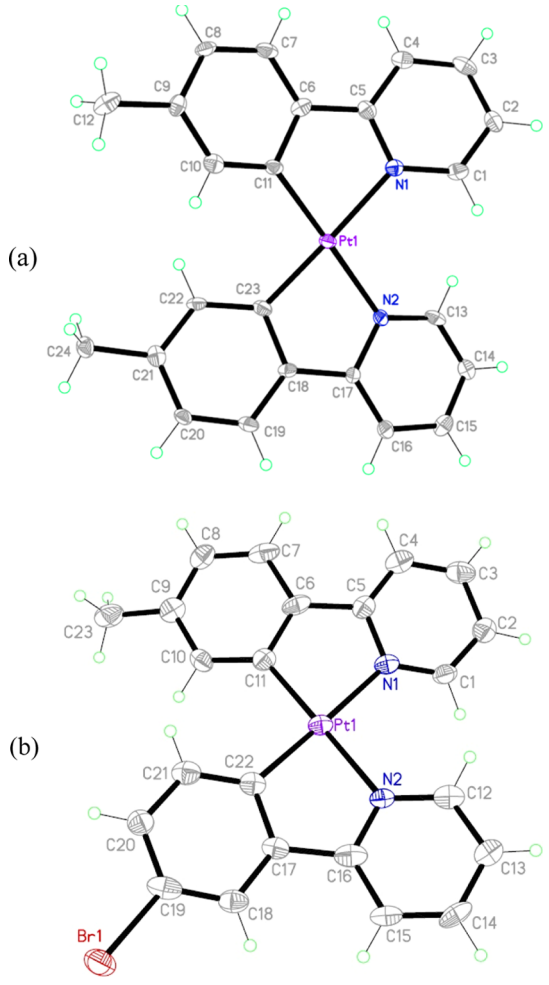

Figure 1. Molecular structures of complex **1** (a) and **2** (b).

cyclometalated ligands in the complexes **1** and **2** have different substituents on the phenyl ring and show different interactions in the solid state. For example, the crystal structure of **1** shows only C–H···π interactions while π···π and Pt···H interactions were observed in the solid-state structure of **2**. These complexes present different packing diagrams caused by the above mentioned interactions (Figure S7a,b). The electrospray ionization (ESI) mass spectra (positive ions mode) of complexes **1** and **2** displayed peaks at m/z 381, 532, 597, 613, (Figures S8–S10) that, according to simulated patterns, are ascribable to the species $[Pt(ptpy)(H_2O)]^+$, $[Pt(ptpy)_2]^+$, $[Pt(ptpy)(bppy)]^+$ and $[Pt(ptpy)(bppy)(H_2O)]^+$, respectively. Complexes **1** and **2** possess an electron-rich platinum center which provides the possibility of preparing new bi- or multinuclear complexes containing Pt–M dative bond units. Thus, we decided to examine the reactivity of bis-cyclometalated complexes **1** and **2** toward Au^I and Tl^I species and to carry out comparative structural and photophysical studies. While reactions of **2** with $TlPF_6$ and $[Au(PPh_3)]^+$ did not yield products that could be characterized, the reaction of **1** with 1 equiv of $TlPF_6$ at room temperature in acetone led to the production of Pt^{II}–Tl^I complex $[Pt(ptpy)_2Tl]PF_6$, **3**, in good yield by the formation of a Pt–Tl dative bond (Scheme 3).

Scheme 3

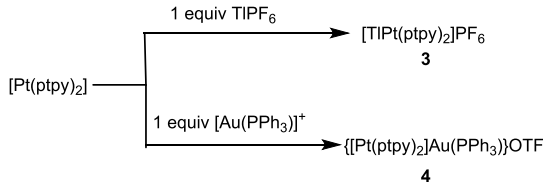

In the ^{1}H NMR spectrum of complex **3** (Figure S11), the appearance of a broad singlet at δ 7.80, flanked by ^{195}Pt satellites ($^3J_{PtH}$ = 52 Hz), was assigned to C–H nuclei adjacent to the coordinated C atoms of the cyclometalated ligands. Four other hydrogen atoms of the phenyl rings appeared as two doublets at δ 7.01 and 7.59 ppm which were correlated to each other in the ^{1}H–^{1}H COSY-DQ NMR spectrum of **3** (Figure S12). A second set of correlations was observed at δ 8.61, 7.48, 8.10, and 7.97 ppm because of hydrogen atoms of the pyridyl rings. The ^{13}C{^{1}H} NMR spectrum is shown in Figure S13. The lack of an observable coupling between Tl and H or C atoms in **3** is not unprecedented and indicates that the Pt–Tl complex is dynamic on the NMR time scale.[6,9] Red needle-like crystals of **3** were obtained by vapor diffusion of *n*-hexane into an acetone solution of **3**. The single-crystal X-ray diffraction analysis revealed that the cation of **3** consists of a helical chain built up from alternate **1** and Tl^I fragments, which are connected by Pt^{II}–Tl^I dative bonds. Figure 2a,b shows views of the asymmetric unit and helical chain along the crystallographic *a*-axis, respectively. One cycle of the helix consists of three bis-cyclometalated platinum complexes and two Tl^I

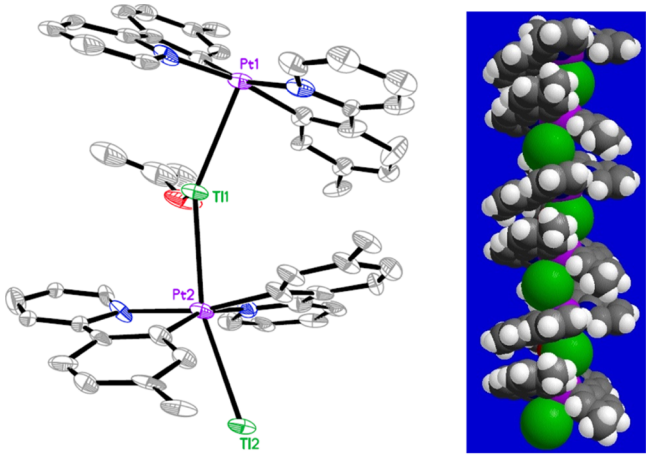

Figure 2. View of asymmetric unit of **3** (a) and its helical chain structure along *a* axis (b). The anions (PF_6), solvents of crystallization and H atoms are omitted for clarity.

DOI: 10.1021/acs.organomet.8b00907
Organometallics XXXX, XXX, XXX–XXX

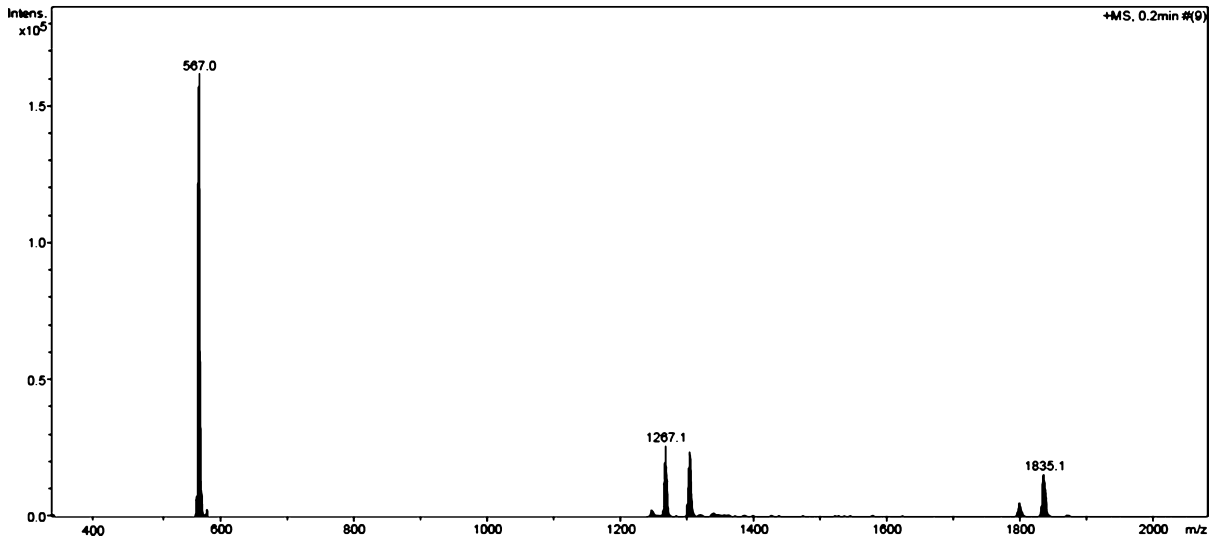

Figure 3. Positive ion mode ESI mass spectrum of **3**.

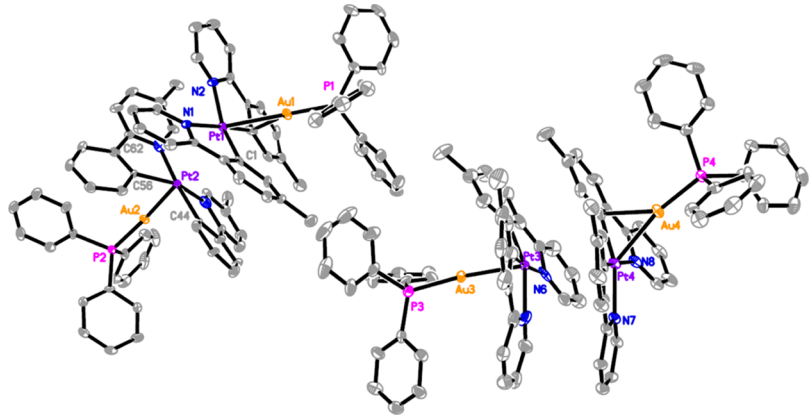

Figure 4. Molecular structure of complex **4**. The OTF anions, solvents of crystallization, and H atoms were omitted for clarity.

metal centers. The pitch of the helix is 11.059 Å, which is equal to the periodicity along the *a*-axis. X-ray structural data (Tables S7−S9) also verified that compound **3** crystalized in achiral space group $P2_1/n$ and the crystals contain both the left- and right-handed helical chains. The asymmetric unit of compound **3** consists of two bis-cyclometalated complexes, **1**, two Tl atoms, a coordinated acetone molecule, and two hexafluorophosphate counterions. The Pt−Tl distances ([2.925(2)−2.974(2) Å]) are in the range of those found in the previously reported helical and linear chains assembled by Pt^{II}−Tl^{I} dative bonds.[6] An interesting feature in the solid-state structure of **3** is the coordination of half the Tl^{I} centers by acetone molecules. This is different from those observed in the solid-state structures of the helical and linear chain compounds $[\{Pt(phpy)_2\}_2\{Ag(acetone)\}_2]_n(ClO_4)_2$,[5] $[\{Pt(bzq)(C_6F_5)_2\}$-$Tl(Me_2CO)]_n$[19] and $[\{Pt(R\text{-}CC^*)(acac)\}_2Tl]PF_6$[20] in which all silver(I) and thallium(I) centers are coordinated by acetone molecules. The coordination of the acetone molecule to Tl1 centers and the C−H···F interactions in the solid state-structure of **3** induce a large separation between two $[Pt(ptpy)_2]$ units connected to Tl1 centers [Pt1−Pt2 distance is 5.7 Å] in comparison with two $[Pt(ptpy)_2]$ units connected to Tl2 centers [Pt1−Pt2 distance is 5.4 Å]. Moreover, the Pt^{II}−Tl^{I} vectors around the Tl1 centers are tilted by 0.9° (Pt1−Tl1) and 4.8° (Pt2−Tl1) with respect to the normal line of the platinum(II) coordination planes which are smaller to those observed around the Tl2 centers [14.4° (Pt1−Tl2) and 13.7° (Pt2−Tl2)]. The Pt1−Tl1−Pt2−Tl2 segments are not linear [Tl1−Pt2−Tl2 162.19(7)°, Tl2−Pt1−Tl1 166.46(7)°, Pt2−Tl2−Pt1 131.35(8)°, Pt1−Tl1−Pt2 153.9°] and the Tl−O bond distance amounts to 2.80(3) Å. An ESI-mass spectrum of **3** (positive ions mode in Figures 3 and S14) is particularly informative and includes peaks at *m*/*z* 1267, 1303, 1798, and 1835 that confirm the formation of heterotrinuclear Pt_2Tl complexes $\{[Pt(ptpy)_2]_2Tl\}^+$, $\{[Pt(ptpy)_2]_2Tl(H_2O)_2\}^+$, and heterotetranuclear Pt_3Tl complexes $\{[Pt(ptpy)_2]_3Tl\}^+$ and $\{[Pt(ptpy)_2]_3Tl(H_2O)_2\}^+$. An example of cyclometalated tetranuclear clusters with a Pt_3Tl metal core has been reported previously.[21]

The reaction of the bis-cyclometalated platinum complex **1** with 1 equiv of $[Au(PPh_3)]OTF$ [prepared in situ from $AuCl(PPh_3)$ and Ag(OTF) in acetone] gave rise to the heterobinuclear Pt^{II}−Au^{I} complex, $\{Pt(ptpy)_2[Au(PPh_3)]\}$-OTF, **4** (Scheme 3). Yellow crystals of **4** were obtained by vapor diffusion of *n*-hexane into a dichloromethane solution of **4**. X-ray diffraction analysis showed that the heterobinuclear complex **4** crystallizes in monoclinic system, with space group $P2_1/c$. A view of the molecular structure of **4** is depicted in Figure 4, and the bond lengths and angles are listed in Tables S10−S12. The asymmetric unit of **4** is composed of four

DOI: 10.1021/acs.organomet.8b00907
Organometallics XXXX, XXX, XXX−XXX

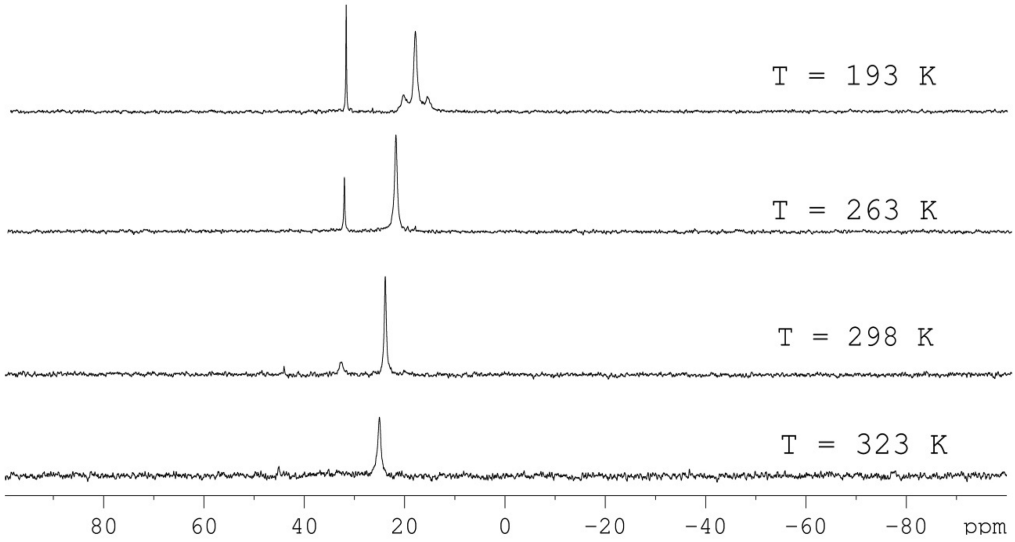

Figure 5. VT $^{31}P\{^{1}H\}$ NMR spectrum of complex **4** in acetone-d_6.

heterobinuclear Pt^{II}–Au^{I} complexes and four triflate counterions.

Each pair of these complexes is linked together by $\pi\cdots\pi$, C–H$\cdots\pi$, and Pt$\cdots$Pt (3.282 and 3.252 Å) interactions and show two different types of Pt–Au bonds: short and long. The long Pt–Au bonds [Pt1–Au1, 2.7311(5) Å, and Pt4–Au4, 2.6457(5) Å] are supported by strong Au–C_{ipso} bonds [Au1–C13 (2.297(9) Å) and Au4–C140, 2.456(9) Å]. However, as far as we know, only one example of this type of unusual Pt–Au bonding has been reported[3] that can be considered as an intermediate for the transmetalation step in bimetallic reactions. The bond distances for the short bonds Pt2–Au2 and Pt3–Au3 amount to 2.5864(5) and 2.552(3) Å, respectively, which are very shorter than those observed in the previously reported Pt^{II}–Au^{I} compounds[22] and are in the range of those observed in the previously reported Pt^{0}–Au^{I} complexes.[23] The ESI-mass spectrum of **4** (Figure S15) shows a base peaks at m/z 990 which confirms the formation of cationic Pt–Au complex $\{Pt(ptpy)_2[Au(PPh_3)]\}^+$. Density functional theory (DFT) calculations on the supported and unsupported Pt–Au bond forms of **4** were performed at the B3LYP level of theory based on experimental geometries. The calculated energy difference between them was 0.9 kcal/mol, in favor of the supported form, indicating the probability of the presence of a dynamic process in solution between these structural forms.

The $^{31}P\{^{1}H\}$ NMR of complex **4** (Figure S16) at 323 K showed a singlet signal at δ 25.1. $^{1}H,^{1}H$-COSY DQ and ^{1}H NMR spectra of **4** (Figures S17 and S18) at the same temperature showed four sets of correlations in the aromatic region (8.87, 7.65, 8.16, and 8.18 ppm for pyridyl rings; 7.81 and 7.18 ppm for *p*-tolyl ring protons, 8.17 ppm for CH groups adjacent to coordinated C atoms; and 7.13, 7.43, and 7.58 for the phenyl protons of the PPh_3 group). The methyl signal was found as a sharp singlet at δ 2.40. Lowering the temperature to 273 K splits the phosphorus singlet signal into two singlet signals at δ 22.8 and 33.0 without platinum satellites (Figures 5). These observations revealed that **4** undergoes a dynamic process in solution. Thus, the $^{31}P\{^{1}H\}$ NMR spectrum of complex **4** was monitored as a function of temperature in the acetone-d_6 solution (Figure 5). A change in the relative intensities and broadness of two phosphorus signals was observed upon cooling from room temperature to 213 K. As the temperature was lowered, the phosphorus resonance at δ 22.8 became more broadened and shifted to upfield, while the phosphorus resonance at δ 33.0 became sharp and did not show any coupling with the platinum atom. Consistently, the $^{31}P\{^{1}H\}$ EXSY NMR spectrum of **4** (Figure 6a) at 213 K in acetone-d_6 showed cross-peaks between two phosphorus resonances. Thus, we suggest that Pt–Au bond in **4** is labile and both of the free and platinum-coordinated forms of $[Au(PPh_3)]^+$ are in a dissociation–association equilibrium (Scheme 4), and the phosphorus resonances observed at δ 33.0 and 23.8 ppm can be assigned to the P atoms of the free and platinum-coordinated fragment $[Au(PPh_3)]^+$, respectively. This is in contrast to the previously reported heterobinuclear Pt–Au(PR_3) complexes that showed only dynamic intramolecular rearrangements.[4,10] A second dynamic process was observed at lower temperature with a platinum-coordinated fragment $[Au(PPh_3)]^+$. When the temperature was decreased to −193 K, signals due to the platinum-coordinated fragment $[Au(PPh_3)]^+$ shifted to downfield and appeared as a singlet signal at δ 18.7 ppm which was coupled to platinum atoms to give satellites with $^{1}J_{PtP}$ = 785 Hz. It is important to note that this resonance does not show correlation with the resonance of the phosphorus atom of the free fragment $[Au(PPh_3)]^+$ in the $^{31}P\{^{1}H\}$ EXSY NMR spectrum of **4** at 193 K (Figure 6b). These NMR data, therefore, show that platinum-coordinated fragment $[Au(PPh_3)]^+$ at 193 K rearranges to a new Pt–Au bond complex that does not dissociate to platinum and gold fragments and persists in solution at this condition. On the basis of the represented NMR data, the crystal structure of **4** and the previously reported cyclometalated Pt^{II}–Au^{I} complex that exhibited persistent of Pt–Au bond in solution,[4] we proposed that Pt-coordinated fragment $[Au(PPh_3)]^+$ forms a strong Au–C_{ipso} bonding interaction in solution at 193 K, as shown in Scheme 4. Inspection of Figure 5 reveals that the ^{31}P NMR signal of **4** at 193 K is not as sharp as one might expect if a blocked conformation for the Pt–Au adduct **4** were present in solution. A possible reason for this can be the migration of the platinum-coordinated fragment $[Au(PPh_3)]^+$ between two C_{ipso} atoms of two ptpy ligands. We have completed the NMR study of **4** in solution by recording ^{1}H and $^{195}Pt\{^{1}H\}$ NMR

DOI: 10.1021/acs.organomet.8b00907
Organometallics XXXX, XXX, XXX–XXX

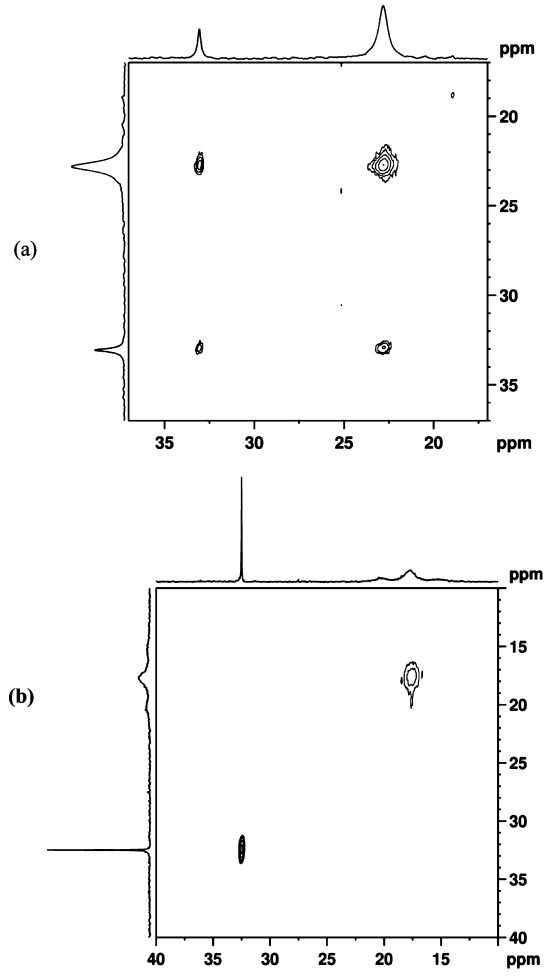

Figure 6. $^{31}P\{^{1}H\}$ EXSY NMR spectrum of **4** in acetone-d_6 at (a) 213 and (b)193 K.

Scheme 4

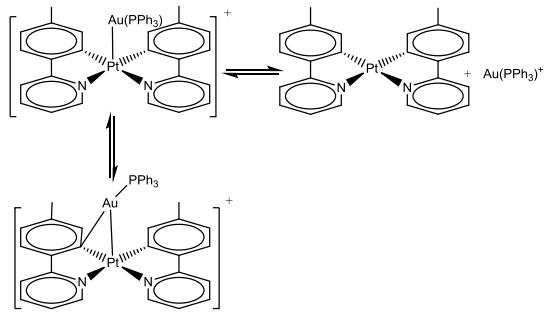

spectra at various temperatures. The dynamic ^{1}H NMR spectra of **4** (Figure 7) showed that at 298 K the PPh_3 proton signals are very broad, while the tolylpyridyl proton signals are relatively sharp. Interestingly, recording the ^{1}H NMR spectrum at 193 K showed very broad signals for the coordinated tolylpyridyl protons and relatively sharp signals for the PPh_3 protons. This is in accord with our hypothesis on the formation, at low T, of a relatively strong Pt−Au bond and a relatively labile C−Au bond, possibly because of a "walking" of the Au from one coordinated C to the other. Consistently, the methyl group protons of the coordinated ptpy show, at 193 K, a broad ^{1}H signal which is compatible with the presence of two unequivalent (albeit almost isochronous) methyl groups in

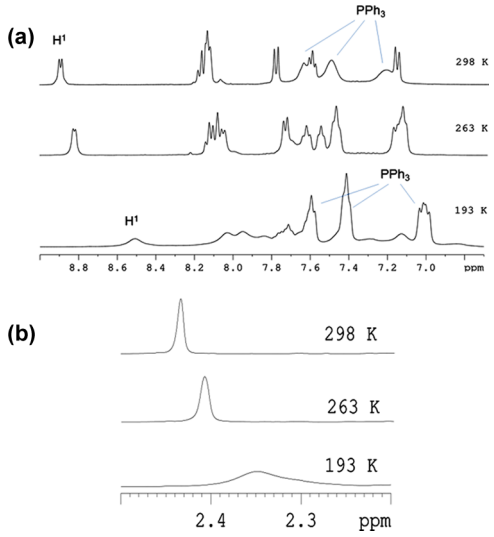

Figure 7. VT ^{1}H NMR spectrum of complex **4** in acetone-d_6 (a) aromatic region (b) methyl region. H^1 is the hydrogen ortho to N of the ptpy ligand.

mutual exchange (Figure 7b). The $^{195}Pt\{^{1}H\}$ NMR spectrum of **4** at 193 K showed a very broad signal at δ −3589 ppm (Figure S20) which is slightly upfield shifted in comparison with that of the starting complex **1** (δ −3553 ppm, Figure S21). No ^{195}Pt NMR signals was found for **4** at 298 or 323 K because of the fast dissociation equilibrium.

Absorption and Emission Spectra. UV−vis absorption spectra of the bis-cyclometalated platinum (II) complexes **1** and **2** were obtained in CH_2Cl_2 solution and in solid state. The obtained spectra are shown in Figure 8a, and the numerical data are summarized in Table 1. The complexes **1** and **2** show UV−vis spectra similar to the previously reported homoleptic bis-cyclometalated complexes $[Pt(ppy)_2]$, $[Pt(bhq)_2]$, $[Pt(thpy)_2]$, $[Pt(bthpy)_2]$,[15a−c,24] and heteroleptic bis-cyclometalated complexes [Pt(thpy)(TMS-thpy)] and [Pt(phpz)(thpy)].[15c,25] Therefore, the intense high-energy absorption bands (λ < 350 nm) and the strong absorption bands in the visible region (420−430 nm) of the UV−vis spectra of **1** and **2** can be ascribed to ^{1}LC (ligand centered) and $^{1}MLCT$ (metal to ligand charge transfer) transitions, respectively. The diffuse reflectance UV−vis spectra of **1** and **2** (Figure 8b) in solid-state show additional bands at low energy region (500 nm) compared with the spectra taken in dichloromethane solution. These additional bands are tentatively attributed to the $\pi\pi^*$ interactions in solid-state structures of **1** and **2** complexes. The electronic absorption spectra of **3** and **4** (Figure S22) in CH_2Cl_2 solution are similar to each other and comparable to that observed for the precursor complex **1**, indicating the dissociation of the Pt−Tl and Pt−Au bonds in solution. However, the UV−vis spectra of **3** and **4** in solid state (Figure S24) show additional low-energy broad bands with long tails to 700 nm reflecting the presence of the Pt−Tl interaction in **3** and Pt−Au, Pt−Pt or π interactions in **4**. Emission data for **1**−**4** are summarized in Table 1. All complexes display long-lived intense emission at room temperature in the solid state. The bis-cyclometalated complexes **1** and **2** are nonemissive in the fluid solution (298 K) but become emissive in the solid state (Figure S24). The emission spectrum of **1** displays a structured band (547_{max}, 298 K and 554_{max}, 77 K), which is typical of the

DOI: 10.1021/acs.organomet.8b00907
Organometallics XXXX, XXX, XXX−XXX

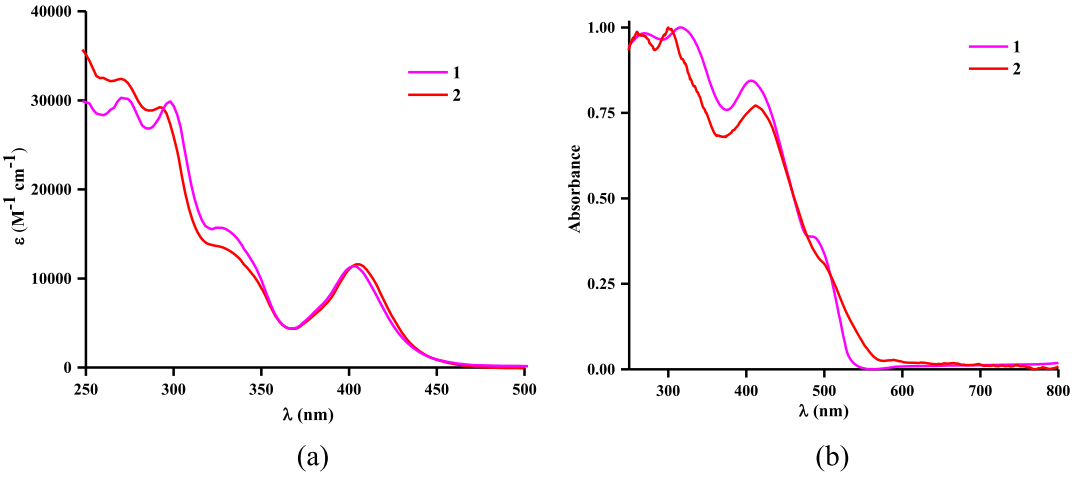

Figure 8. (a) Absorption spectra in CH_2Cl_2 (concentration = 5×10^{-5} M) and (b) diffuse reflectance UV−vis spectra in the solid state of complexes **1** and **2** at 298 K.

Table 1. Absorption and Emission Data for 1−5

complexes	λ_{abs}/nm (10^4 ε M^{-1} cm^{-1})	λ_{em}/nm (λ_{exc}/nm)[c]	τ (μs)[d]	ϕ[e]
1	272(3.0), 298 (2.9), 329 (1.6), 385_{sh} (0.7), 403 (1.2) **CH_2Cl_2**[a]	530, 547_{max}, 596_{sh} (365−500), 298 K	14.2, 298 K	0.21
	269, 316, 409 **solid**[b]	532, 554_{max}, 597_{sh} (380−500), 77 K	20.4, 77 K	
2	271 (3.2), 293 (2.9), 337 (1.2), 383_{sh} (0.6), 406 (1.2) **CH_2Cl_2**[a]	622 (400−440), 298 K	10.1, 298 K	0.09
	264, 302, 412 **solid**[b]	610 (380−480), 77 K	13.9, 77 K	
3	273 (2.1), 296 (1.8), 311 (1.6), 351 (0.7), 397 (0.6) **CH_2Cl_2**[a]	640 (400−460), 298 K	12.3, 298 K	0.11
	271, 317, 402, 481 tail to 645 **solid**[b]	663 (400−480), 77 K	18.6, 77 K	
4	271 (1.1), 297 (0.8), 326 (0.3), 349 (0.2), 403 (0.2) **CH_2Cl_2**[a]	592 (360−420), 298 K	8.8, 298 K	0.10
	323, 414, 494 tail to 630 **solid**[b]	614 (380−450), 77 K	13.1, 77 K	

[a]In CH_2Cl_2 solution (5×10^{-5} M) at 298 K. [b]Diffuse Reflectance in solid state at 298 K. [c]Highest-energy emission peak in solid state. [d]Emission lifetime. [e]Absolute quantum yield in solid state at 298 K.

mononuclear cyclometalated platinum complexes and is assigned to an admixture of ^{3}IL/^{3}MLCT excited states.[26]

This band in the emission spectrum of **2** is structureless and red-shifted (622 nm) compared with its counterpart observed in the emission spectrum of **1** (Figure S25). Complexes **3** and **4** show phosphorescent emissions in solid state with excited-state lifetimes in microsecond scale (12.3 μs, **3** and 8.7 μs, **4**) and quantum yields of 11 and 6%, respectively. Figure 9a,b shows the luminescence spectra of **3** and **4** measured at room temperature and 77 K that display structureless low energy bands at λ_{max} = 640 and 592 nm, respectively. The latter displays a high energy shoulder at λ = 530 nm, and its intensity decreases by lowering the temperature down to 77 K. The photophysical properties of **3** and **4** were investigated by time-dependent DFT calculations (PBE0-TDDFT). The singlet excitation spectra of the complexes at their optimized ground-state geometries were calculated. The geometries of the lowest-energy triplet states were then optimized to investigate their emission features. The calculated photophysical data are listed in Table 2, and the excited state transition densities are shown in Figure 10.

For complex **3**, the calculated $S_0 \rightarrow S_1$ excitation energy is in good agreement with the experimental absorption data. The computational data show that the lowest-energy excitation $S_0 \rightarrow S_1$ is a LMCT transition with a transfer of electron density from platinum metal centers to ptpy ligands. As shown in Figure 10, the nature of the lowest-energy singlet excitations of the Pt−Au complexes with and without supported Au−C_{ipso} bond are similar to that observed in **3**. The calculated $T_1 \rightarrow S_0$ emission energies are also in line with the experimental results. For the lowest-energy triplet emission in **3**, the contribution of the thallium and platinum atoms becomes more significant and the emission is associated with the Pt−Tl chromophore.[19,27] This emission band slightly red-shifted at 77 K (663 nm) because of the shorter Pt−Tl distance at low temperature.[6a,c,19] However, there is notable difference in the electron density transition for the lowest triplet emissions $T_1 \rightarrow S_0$ of the two structural forms of **4**. In the case of the Pt−Au complex with the supported Au−C_{ipso} bond, the transition density is mostly centered on the ptpy ligands and platinum atom (MLCT contribution), while the gold atoms play a minor role. On the other hand, for the Pt−Au complex without the supported Au−C_{ipso} bond, the ptpy ligands play only a minor role and the triplet emission is actually centered on the gold and platinum atom centers. These computational data are in good agreement with those observed in the emission (at 298 and 77 K), variable temperature ^{31}P NMR and EXSY spectra of **4**. As the temperature decreases from 298 K to low temperatures, the intensity of the shoulder band at 530 nm decreases (Figure 9b) and the EXSY, and ^{31}P NMR spectra show the conversion of unsupported Pt−Au bond form to supported Pt−Au bond form of **4** (Figures 5 and 6). We therefore suggest that the emission band observed at λ_{max} = 592 nm and its shoulder at 530 nm can be attributed to the presence of two structural forms of **4**, with and without Au−C_{ipso} bonding interaction, respectively.

DOI: 10.1021/acs.organomet.8b00907
Organometallics XXXX, XXX, XXX−XXX

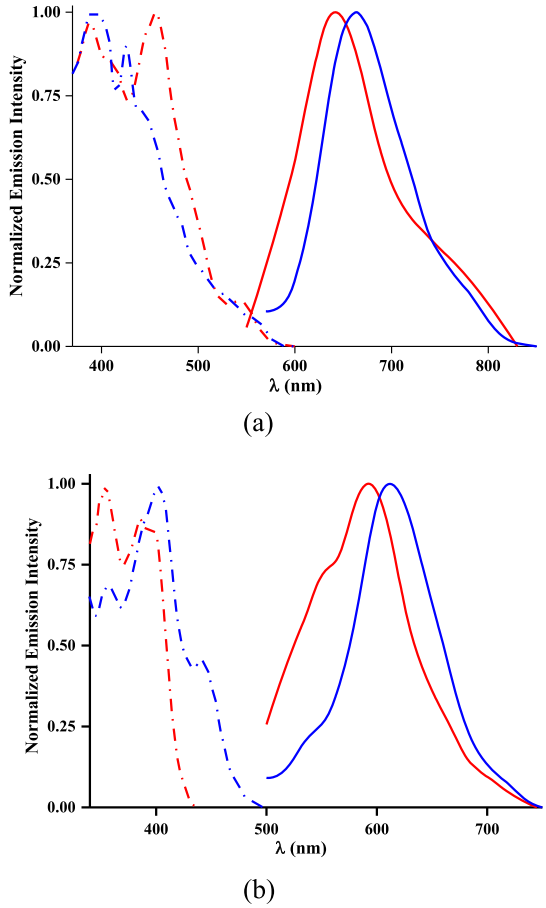

Figure 9. (a) Normalized excitation and emission spectra of complex **3** in solid states at 298 K (red) and at 77 K (blue) (λ_{exc} 440 nm). (b) Normalized excitation and emission spectra of complex **4** in the solid state at 298 K (red) and at 77 K (blue) (λ_{exc} 400 nm).

Table 2. Calculated Photophysical Results for 3 and 4

	λ_{ab} $S_0 \rightarrow S_1$ (nm)		λ_{em} $T_1 \rightarrow S_0$ (nm)	
complex	cal	exp	cal	exp
3	409	397	602	640
4	(with Au−C bond)	322[a]	523	530
4	(without Au−C bond)	351[a]	549	592

[a]Complexes **3** and **4** undergo dissociation in solution.

CONCLUSION

The biscyclometalated platinum(II) complexes **1** and **2** have been prepared using a new synthetic method, and their crystal structures have been determined by X-ray crystallography. Different packing patterns in the solid state have been observed which is due to the different substituents on the phenyl rings. The reaction of **1** with Tl^I and Au^I species gave rise to the formation of the infinite helical chain $[-Pt^{II}-Tl^I-]_\infty$ compound **3** and the heterobinuclear $Pt^{II}-Au^I$ complex **4**, respectively. The solid-state structure of **4** displayed two different short and long $Pt^{II}-Au^I$ bonds. The length of the short bonds were in the range of Pt^0-Au^I bonds, while the long bonds were supported by strong Au−C_{ipso} bonds. In contrast to the previously reported $Pt^{II}-Au^I(PR_3)$ complexes[4,10,12] that show less labile $Pt^{II}-Au^I$ bond and undergo intramolecular dynamic processes, NMR spectroscopy showed that complex **4** has a $Pt^{II}-Au^I$ labile bond at room temperature

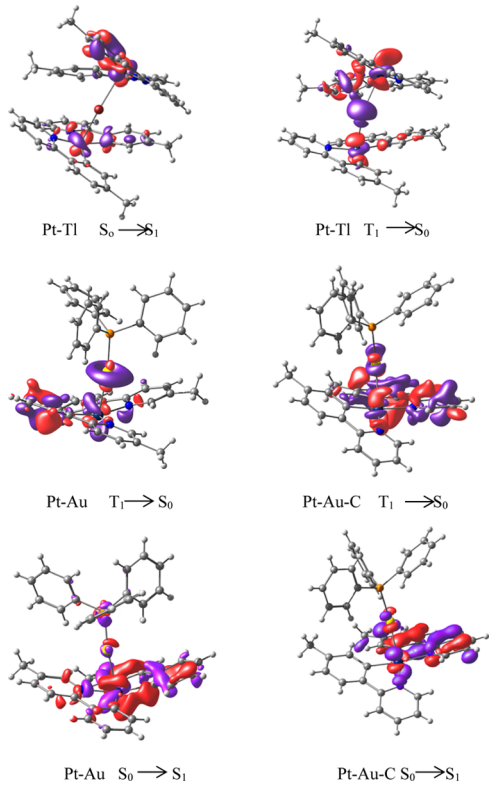

Figure 10. PBE0-DFT transition densities for the lowest-energy singlet excitations and triplet emissions of **3** and **4**. During the electronic transition, the electron density increases in the blue areas and decreases in the red areas.

and undergoes a dissociation−association equilibrium in solution and a second dynamic process at low temperature between supported and unsupported Pt−Au bond forms of **4**. The heterobinuclear complexes **3** and **4** exhibit bright red and orange emissions in solid state, respectively. Although the emission of complex **3** originated from a triplet excited state with a Pt−Tl character, the emission band in complex **4** is associated with a high energy shoulder which is due to supported and unsupported Pt−Au bond forms of **4**. Calculation data show that intense band due to supported Pt−Au bond form originated from an excited state that concentrate on Au and Pt metal centers while the shoulder band due to unsupported Pt−Au bond form originated from an ^{3}MLCT excited state.

EXPERIMENTAL SECTION

The ^{1}H, ^{13}C{1H}, ^{31}P{^{1}H}, ^{195}Pt, and 2D NMR spectra were recorded using Bruker AVANCE DRX 500-MHz Bruker and DPX-400 spectrometers. The operating frequencies and references, respectively, are shown in parentheses as follows: ^{1}H (TMS), ^{13}C (TMS), ^{31}P (85% H_3PO_4), and ^{195}Pt (Na_2PtCl_6). The chemical shifts and coupling constants are in ppm and Hz, respectively. The UV−vis absorption spectra were carried out in a Hewlett-Packard 8453 spectrophotometer. Diffuse reflectance UV−vis (DRUV) data of the pressed powders were recorded on a UV−vis−NIR spectrometer Cary 5-E (Varian). Photoluminescence spectra were recorded on a PerkinElmer LS45 fluorescence spectrometer at room and low temperatures and the lifetimes were measured in phosphorimeter mode. 2-(*p*-tolyl)pyridine, 2-(3-bromophenyl)pyridine, and $TlPF_6$ were purchased from commercial sources. $[Pt_2Me_4(\mu\text{-}SMe_2)_2]$,[28] $[AuCl(PPh_3)]$,[29] and $[Pt(2\text{-}(p\text{-tolyl})pyridine)Me(SMe_2)]$[17] were prepared as described previously. Geometry optimizations without

DOI: 10.1021/acs.organomet.8b00907
Organometallics XXXX, XXX, XXX−XXX

symmetry constraints were carried out by using the BP86 functional in conjunction with the D3 dispersion correction suggested by Grimme and co-workers.[30] Platinum, gold, and thallium atoms were described using the scalar-relativistic Stuttgart−Dresden SDD effective core potentials and their associated double-ξ basis sets. The 6-31G(d) basis set was used for C, H, N, and P atoms. This level is denoted BP86-D3/6-31G(d) & SDD+f(Pt, Au). The photophysical properties of **3** and **4** were investigated by TDDFT calculations (PBEPBE-TDDFT). The Au, Pt, and Tl atoms were described by a triple-valence-zeta quality basis set with polarization functions (def2-TZVP). The 6-31G(d) basis set was used for C, H, N, and P atoms. The geometries of the complexes were taken from the solid-state X-ray structures. All electronic-structure calculations and geometry optimizations were performed with the Gaussian 09 suite of programs.

Crystal Structure Determinations. X-ray intensity data for **1**−**3** were collected using the full sphere routine by φ and ω scans strategy on a SMART APEX2 Bruker diffractometer. Intensity data were collected a Bruker SMART CCD single-crystal diffractometer with graphite-monochromated Mo Kα radiation (λ = 0.71073 A). Frames were integrated with the SAINT program [**SAINT Program Version4, 1994−1996; 6300 Interprise Lane, Madison, WI53719**]. Routine LP correction based upon SADABS was applied to the intensity data. X-ray intensity data for 4 Agilent SuperNova dual wavelength EoS S2 diffractometer with mirror monochromated with Cu Kα (1.54184 Å) and Mo Kα radiation (λ = 0.71073 Å). For all data collections, the crystals were cooled to 150 K using an Oxford diffraction Cryojet low-temperature attachment. The data reduction, including an empirical absorption correction using spherical harmonics, implemented in *SCALE3 ABSPACK* scaling algorithm[31] was performed using the *CrysAlisPro* software package.[32] The crystal structures were solved by direct methods using the online version of *AutoChem 2.0* in conjunction with *OLEX2* suite of programs implemented in the *CrysAlis* software.[33,34] The structures were refined by full-matrix least-squares (*SHELXL2014-7*) on F^2.[35] The nonhydrogen atoms were refined anisotropically. All hydrogen atoms were positioned geometrically in idealized positions and were refined with the riding model approximation, with U_{iso}(H) = 1.2 or 1.5 U_{eq}(C). For molecular graphics, the SHELXTL program was used.[35] All geometric calculations were carried out using the *PLATON* software.[36] Crystallographic data for the structural analysis has been deposited with the Cambridge Crystallographic Data Centre, no. CCDC-1826422 (**1**), CCDC-1826421 (**2**), CCDC-1826423 (**3**), and CCDC-1826424 (**4**). In structure **1**, the reflection (2 0 0) was affected by beam stop and its contribution to the structure factor was omitted from the refinement cycle. In the case of structure **2**, there was a large electron density peak (4.2 e·Å^{-3}) near to C8 and C23 carbon atoms of the phenyl ring. We checked the data for merohedral and nonmerohedral twinning to explain the presence of such high electron density peak but no sign of twinning was observed. The disorder modeling of Br atom was not correct to fit into a reasonable model; therefore, it might be due to the systematic errors. The crystal of **3** was not diffracting enough to get reasonable resolution for its data. The crystal was not optimal with a cracked surface, and even after successive crystallization, it was not possible to obtain a high-quality single crystal for X-ray analysis. For structure **3**, we used a global SIMU and DELU restraints to get a better model for ellipsoids. We also applied EADP for second PF_6 counter ion to be the same as first one. The EADP command was also applied to some carbon atoms of the ring. In the case of structure **4**, the crystal was brittle and had cracks even after successive crystallization, preventing us from obtaining its optimal single crystal. The diffraction limit of the crystal was also low; thus, we had to use lots of different restraints to model the structure. The structure was squeezed with a squeeze routine (version 280317) [**A. L. Spek, PLATONSQUEEZE: a tool for the calculation of the disordered solvent contribution to the calculated structure factors, ActaCryst.(2015). C71, 9−18.**] in PLATON which showed significant solvent-accessible voids of 1039 electrons in the cell, confirming losing a lot of dichloromethane and acetone molecules as solvent of crystallization. We used a global SIMU and DELU restraints to get a better model based on ellipsoids shape. We also tried to apply whole molecule disorder for the phenylpyridine ligands coordinated to Pt3, but the refinement of the modeling was not stable and successful. With such low-resolution data we could not do better to get a reasonable structure. For structure **4**, in one of the Pt−Au complexes in the asymmetric unit, the Pt3 atom was disordered in two positions with refined site occupancies 0.778(8)/0.222(8). The Au atom of the same complex was also disordered over two positions with a refined site occupancy ratio 0.650(14)/0.350(14). On the other hand, one of the triflate counterions was totally disordered over two positions with a refined site occupancy ratio of 0.645(14)/0.355(14).

[Pt(ptpy)(bppy)], 2. To a solution of the complex {PtMe[2-(*p*-tolyl)pyridine](SMe$_2$)} (100 mg, 0.227 mmol) in acetone (15 mL) 1 equiv of 2-(3-bromophenyl)pyridine (53.1 mg, 0.227 mmol) was added at room temperature. The mixture was stirred and bubbled with argon gas for 5 h to remove SMe_2 from solution. Then, 1 equiv of $B(C_6F_5)_3$ (116.2 mg, 0.227 mmol) was added, and the solution was further stirred for 2 h. A bright yellow solution was formed, the solvent was removed under reduced pressure, and the residue was triturated with ether. The product as an orange solid was dried under vacuum. Yield: 40%. Anal. Calcd for $C_{23}H_{17}N_2BrPt$: C, 46.3; H, 2.8; N, 4.7. Found: C, 46.1; H, 2.9; N, 4.9. NMR data in $CDCl_3$: δ(^{1}H) 8.8 (d, $^3J_{HH}$ = 5.8 Hz, 1H), 8.74 (d, $^3J_{HH}$ = 5.8 Hz, 1H), 8.07(d, $^3J_{HH}$ = 8 Hz, $^3J_{PtH}$ = 49 Hz, 1H), 7.8−7.9 (m, 4H), 7.76 (d, J_{HH} = 2 Hz, 1H), 7.55 (d, $^3J_{HH}$ = 8 Hz, 1H), 7.44 (dd, J_{HH} = 8 and 3 Hz, 1H), 7.35 (t, 1H), 7.28 (t, 1H), 6.99 (d, $^3J_{HH}$ = 8 Hz, 1H), 2.45 (s, 3H). δ (^{13}C) 166, 165, 148.4, 147.7, 147.5, 146.9, 146.5, 143.5, 140.1, 139, 138, 137.9, 132.5, 126.2, 124.4, 123.4, 122.7, 121.7, 119.4, 119, 116.9, 21.8.

The reactions of the complexes {PtMe[2-(*p*-tolyl)pyridine](SMe$_2$)} with 2-(*p*-tolyl)pyridine and $B(C_6F_5)_3$ using the same conditions and workup procedures as above led to the formation of **1** as orange solid, which was isolated in 50% yield, respectively. The NMR spectra of **1** are the same as reported previously.

[Pt(ptpy)$_2$Tl]PF$_6$, 3. To a solution of complex **1** (200 mg, 0.376 mmol) in acetone (20 mL) at room temperature under an argon atmosphere was added 1 equiv of $TlPF_6$ (131.4 mg, 0.376 mmol). The mixture was stirred at this condition for 1 h, and the solvent was removed thereafter under reduced pressure. The residue was washed with ether, and the red product was dried under vacuum. Yield: 60%. Anal. Calcd for $C_{24}H_{20}N_2F_6PTlPt$: C, 32.7; H, 2.3; N, 3.2. Found: C, 32.5; H, 2.4; N, 3.4. NMR data in $CDCl_3$: δ(^{1}H) 8.61(d, $^3J_{HH}$ = 6 Hz, 2H, CH groups adjacent to coordinated N atoms), 8.1 (t, 2H, CH groups on the pyridyl rings), 7.97 (d, $^3J_{HH}$ = 7 Hz, 2H, CH groups on the pyridyl rings), 7.8 (s, $^3J_{PtH}$ = 52 Hz, 2H, CH groups adjacent to coordinated C atoms) 7.59 (d, $^3J_{HH}$ = 7 Hz, 2H, CH groups on the *p*-tolyl rings), 7.48 (t, 2H, CH groups on the pyridyl rings), 7.01(d, $^3J_{HH}$ = 7 Hz, 2H, CH groups on the *p*-tolyl rings), 2.39 (s, 6H, CH_3 groups on the *p*-tolyl rings), δ(^{13}C) 165.1 (coordinated C atoms), 148.3, 145.6, 143.7, 139.7 (J_{PtC} = 72 Hz), 139.2, 137.4 (J_{PtC} = 96 Hz), 125.1, 124.2 (J_{PtC} = 39.2 Hz), 122.8, 119.5, 21.1.

[Pt(ptpy)$_2$Au(PPh$_3$)]OTF, 4. To a solution of complex **1** (200 mg, 0.376 mmol) in acetone (20 mL) at room temperature under an argon atmosphere was added 1 equiv of [Au(PPh_3)]OTF [prepared from Au(PPh_3)Cl and 1 equiv AgOTF]. The mixture was stirred at this condition for 1 h in the dark, and then, the solvent was removed under reduced pressure. The residue was washed with ether, and the red product was dried under vacuum. Yield: 75%. $C_{43}H_{35}F_3N_2PSO_3PtAu$: C, 45.3; H, 3.0; N, 2.5. Found: C, 45.0; H, 3.2; N, 2.8. NMR data in acetone-d_6: δ (^{1}H, 305 K) 8.87 (d, $^3J_{HH}$ = 5 Hz, 2H, CH groups adjacent to coordinated N atoms), 8.09−8.25 (m, 4H, CH groups on the pyridyl rings, 2H and CH groups adjacent to coordinated C atoms), 7.82 (d, $^3J_{HH}$ = 8.1 Hz, 2H, CH groups on the *p*-tolyl rings), 7.65 (t, 2H, CH groups on the pyridyl rings), 7.57 (t, 3H, CH groups on the phenyl rings of PPh_3), 7.43 (t, 6H, CH groups on the phenyl rings of PPh_3), 7.18 (t, 6H, CH groups on the phenyl rings of PPh_3), 7.14 (d, $^3J_{HH}$ = 8 Hz, CH groups on the *p*-tolyl rings), δ (^{13}C, 305 K) 164.5 (coordinated C atoms), 149, 146.6, 140.5, 140, 133.5 (d, J_{PC} = 15 Hz, C atoms of PPh_3 group), 132.2 (d, J_{PC} = 2.6 Hz, C atoms of PPh_3 group), 129.4(d, J_{PC} = 12 Hz, C atoms of PPh_3 group), 128.9, 128.3, 127.7, 125 (J_{PtC} = 30 Hz), 123.7, 120 (J_{PtC} = 20

DOI: 10.1021/acs.organomet.8b00907
Organometallics XXXX, XXX, XXX−XXX

Hz), 21. δ (^{31}P, 323 K) 25.4 (s, broad). δ (^{195}Pt, 193 K) −3589 (broad).

■ ASSOCIATED CONTENT

Supporting Information

The Supporting Information is available free of charge on the ACS Publications website at DOI: 10.1021/acs.organomet.8b00907.

^{1}H NMR, ^{13}C{^{1}H} NMR, and 2D(^{1}H,^{1}H) COSY-DQ NMR spectrum of **1** in $CDCl_3$; ^{1}H NMR, ^{13}C NMR, (^{1}H,^{1}H)-COSY-DQ-NMR, ESI-MASS, and expansion of ESI-MASS spectrum of **2**; crystal packing diagrams of **1** and **2**; ESI-MASS spectrum (positive mode) of **1**; ^{1}H NMR, 2D(^{1}H,^{1}H) COSY-DQ NMR, and ^{13}C{^{1}H} NMR spectrum of **3**; expansion of ESI mass spectrum of **3** and simulated spectrum; ESI-MASS, ^{31}P{^{1}H} NMR, 2D(^{1}H,^{1}H) COSY-DQ NMR, ^{1}H NMR, and ^{13}C{^{1}H} NMR spectrum of **4**; ^{195}Pt NMR spectrum of **1** and **4**; absorption spectra and normalized diffuse reflectance UV−vis spectra of complexes **3** and **4**; normalized excitation and emission spectra; and molecular structures of **1**, **2**, and **3** (PDF)

Molecule geometry (XYZ)

Accession Codes

CCDC 1826421−1826424 contain the supplementary crystallographic data for this paper. These data can be obtained free of charge via www.ccdc.cam.ac.uk/data_request/cif, or by emailing data_request@ccdc.cam.ac.uk, or by contacting The Cambridge Crystallographic Data Centre, 12 Union Road, Cambridge CB2 1EZ, UK; fax: +44 1223 336033.

■ AUTHOR INFORMATION

Corresponding Author

*E-mail: sjamali@sharif.ir.

ORCID

Sirous Jamali: 0000-0002-5997-2619

Reza Kia: 0000-0001-7178-0049

Hamidreza Samouei: 0000-0003-4125-9556

Piero Mastrorilli: 0000-0001-8841-458X

Hamid R. Shahsavari: 0000-0002-2579-2185

Paul R. Raithby: 0000-0002-2944-0662

Notes

The authors declare no competing financial interest.

■ ACKNOWLEDGMENTS

We thank Sharif University of Technology Research Council (grant no. G930615) and Iran national scince foundation (grant no. 96017102) for the financial support. R.K. thanks P.R.R. and Bath University for visiting research scientist position and provided facilities. P.R.R. is grateful to the Engineering and Physical Sciences Research Council (EPSRC) for continued funding (EP/K004956/1). This paper is dedicated in memory of Professor Mehdi Rashidi.

■ REFERENCES

(1) Puddephatt, R. J. Compounds with Platinum-Metal Bonds: A Personal Account. *J. Organomet. Chem.* **2017**, *849−850*, 268−278.

(2) (a) Casares, J. A.; Espinet, P.; Fuentes, B.; Salas, G. Insights into the Mechanism of the Negishi Reaction: ZnRX versus ZnR_2 Reagents. *J. Am. Chem. Soc.* **2007**, *129*, 3508−3509. (b) delPozo, J.; Gioria, E.; Casares, J. A.; Álvarez, R.; Espinet, P. Organometallic Nucleophiles and Pd: What Makes $ZnMe_2$ Different? Is Au Like Zn? *Organometallics* **2015**, *34*, 3120−3128. (c) del Pozo, J.; Salas, G.; Álvarez, R.; Casares, J. A.; Espinet, P. The Negishi Catalysis: Full Study of the Complications in the Transmetalation Step and Consequences for the Coupling Products. *Organometallics* **2016**, *35*, 3604−3611. (d) Carrasco, D.; Pérez-Temprano, M. H.; Casares, J. A.; Espinet, P. Cross Alkyl-Aryl versus Homo Aryl-Aryl Coupling in Palladium-Catalyzed Coupling of Alkyl-Gold(I) and Aryl-Halide. *Organometallics* **2014**, *33*, 3540−3545. (e) Casado, A. L.; Espinet, P. A Novel Reversible Aryl Exchange Involving Two Organometallics: Mechanism of the Gold(I)-Catalyzed Isomerization of *trans*-[PdR_2L_2] Complexes (R = Aryl, L = SC_4H_8). *Organometallics* **1998**, *17*, 3677−3683.

(3) (a) Oeschger, R. J.; Chen, P. Structure and Gas-Phase Thermochemistry of a Pd/Cu Complex: Studies on a Model for Transmetalation Transition States. *J. Am. Chem. Soc.* **2017**, *139*, 1069−1072. (b) Moret, M.-E.; Serra, D.; Bach, A.; Chen, P. Transmetalation Supported by a Pt^{II}-Cu^{I} Bond. *Angew. Chem., Int. Ed.* **2010**, *49*, 2873−2877. (c) Oeschger, R. J.; Chen, P. The First Heterobimetallic Pd-Zn Complex: Study of a d^8−d^{10} Bond in Solid State, in Solution, and in Silico. *Organometallics* **2017**, *36*, 1465−1468.

(4) (a) Baya, M.; Belío, Ú.; Fernández, I.; Fuertes, S.; Martín, A. Unusual Metal-Metal Bonding in a Dinuclear Pt-Au Complex: Snapshot of a Transmetalation Process. *Angew. Chem., Int. Ed.* **2016**, *55*, 6978−6982. (b) Baya, M.; Belío, Ú.; Campillo, D.; Fernández, I.; Fuertes, S.; Martín, A. Pt-M Complexes (M=Ag, Au) as Models for Intermediates in Transmetalation Processes. *Chemistry*. **2018**, *24*−13879. DOI: 10.1002/chem.201802542

(5) Yamaguchi, T.; Yamazaki, F.; Ito, T. A Helical Metal−Metal Bonded Chain via the Pt→Ag Dative Bond. *J. Am. Chem. Soc.* **2001**, *123*, 743−744.

(6) (a) Falvello, L. R.; Forniés, J.; Garde, R.; García, A.; Lalinde, E.; Moreno, M. T.; Steiner, A.; Tomás, M.; Usón, I. Tri-[Pt_2Tl]$^{3-}$ and Polynuclear Chain [Pt-Tl]$_\infty^-$ Complexes Based on Nonbridged Pt^{II}-Tl^{I} Bonds: Solid State and Frozen Solution Photophysical Properties. *Inorg. Chem.* **2006**, *45*, 2543−2552. (b) Berenguer, J. R.; Lalinde, E.; Martín, A.; Moreno, M. T.; Sánchez, S.; Shahsavari, H. R. Binuclear Complexes and Extended Chains Featuring Pt^{II}-Tl^{I} Bonds: Influence of the Pyridine-2-Thiolate and Cyclometalated Ligands on the Self-Assembly and Luminescent Behavior. *Inorg. Chem.* **2016**, *55*, 7866−7878. (c) Forniés, J.; García, A.; Lalinde, E.; Moreno, M. T. Luminescent One- And Two-Dimensional Extended Structures and a Loosely Associated Dimer Based on Platinum(II)-Thallium(I) Backbones†. *Inorg. Chem.* **2008**, *47*, 3651−3660. (d) Forniés, J.; Fuertes, S.; Martín, A.; Sicilia, V.; Gil, B.; Lalinde, E. Extended structures containing Pt(II)-Tl(I) bonds. Effect of these interactions on the luminescence of cyclometalated Pt(II) compounds. *Dalton Trans.* **2009**, 2224−2234.

(7) Jamali, S.; Ashtiani, M. M.; Jamshidi, Z.; Lalinde, E.; Moreno, M. T.; Samouei, H.; Escudero-Adán, E.; Benet-Buchholz, J. A Highly Efficient Luminescent Pt_2Tl_2 Chain with a Short Tl^{I}-Tl^{I} Interaction. *Inorg. Chem.* **2013**, *52*, 10729−10731.

(8) (a) McArdel, C. P.; Vittal, J. J.; Puddephatt, R. J. *Angew. Chem.* **2000**, *39*, 3819−3822. (b) Coker, N. L.; Krause Bauer, J. A.; Elder, R. C. Emission Energy Correlates with Inverse of Gold−Gold Distance for Various [Au(SCN)2]-Salts. *J. Am. Chem. Soc.* **2004**, *126*, 12−13. (c) Zhang, X.; Chi, Z.; Zhang, Y.; Liu, S.; Xu, J. Recent advances in mechanochromic luminescent metal complexes. *J. Mater. Chem. C* **2013**, *1*, 3376−3390. (d) Catalano, V. J.; Malwitz, M. A.; Noll, B. C. Pd(0) and Pt(0) Metallocryptands Encapsulating a Spinning Mercurous Dimer. *Inorg. Chem.* **2002**, *41*, 6553−6559. (e) Jobbágy, C.; Baranyai, P.; Marsi, G.; Rácz, B.; Li, L.; Naumov, P.; Deák, A. Novel gold(i) diphosphine-based dimers with aurophilicity triggered multistimuli light-emitting properties. *J. Mater. Chem. C* **2016**, *4*, 10253−10264.

(9) (a) Catalano, V. J.; Bennett, B. L.; Kar, H. M.; Noll, B. C. Synthesis and Characterization of Trigonal Gold(I) Cage Complexes: Luminescent Metallocryptates Encapsulating Tl(I) and Na^+ Ions. *J. Am. Chem. Soc.* **1999**, *121*, 10235−10236. (b) Catalano, V. J.; Bennett, B. L.; Yson, R. L.; Noll, B. C. Synthesis and Characterization

DOI: 10.1021/acs.organomet.8b00907
Organometallics XXXX, XXX, XXX−XXX

of Pd(0) and Pt(0) Metallocryptands Encapsulating Tl^+ Ion. *J. Am. Chem. Soc.* **2000**, *122*, 10056−10062. (c) Catalano, V. J.; Bennett, B. L.; Muratidis, S.; Noll, B. C. Unsupported Pt(0)−Tl(I) Bonds in the Simple [Pt(PPh2Py)3Tl]+Complexes. *J. Am. Chem. Soc.* **2001**, *123*, 173. (d) Catalano, V. J.; Malwitz, M. A. Mixed-Metal Metallocryptands. Short Metal−Metal Separations Strengthened by a Dipolar Interaction. *J. Am. Chem. Soc.* **2004**, *126*, 6560.

(10) (a) Alonso, E.; Forniés, J.; Fortuño, C.; Lledós, A.; Martín, A.; Nova, A. Behavior of P−Pt and P−Pd Bonds in Phosphido Complexes toward Electrophilic Fragments§. *Inorg. Chem.* **2009**, *48*, 7679−7690. (b) Forniés, J.; Fortuño, C.; Ibáñez, S.; Martín, A.; Mastrorilli, P.; Gallo, V. Behavior of Neutral Phosphido Derivatives of Platinum and Palladium toward Silver Centers. *Inorg. Chem.* **2011**, *50*, 10798−10809.

(11) (a) Arias, A.; Forniés, J.; Fortuño, C.; Martín, A.; Mastrorilli, P.; Gallo, V.; Latronico, M.; Todisco, S. Donor Behaviour of Anionic and Asymmetric Phosphanido Derivatives of Platinum and Palladium. *Eur. J. Inorg. Chem.* **2014**, 1679−1693. (b) Latronico, M.; Sánchez, S.; Rizzuti, A.; Gallo, V.; Polini, F.; Lalinde, E.; Mastrorilli, P. Reactivity of the phosphinito bridged Pt(i) complex [(PHCy2)Pt(μ-PCy2)-{κ2P,O-μ-P(O)Cy2}Pt(PHCy2)](Pt-Pt) towards Au(i) and Ag(i) electrophiles. *Dalton Trans.* **2013**, *42*, 2502−2511.

(12) Juliá, F.; Jones, P. G.; González-Herrero, P. Synthesis and Photophysical Properties of Cyclometalated Platinum(II) 1,2-Benzenedithiolate Complexes and Heterometallic Derivatives Obtained from the Addition of [Au(PCy3)]+ Units. *Inorg. Chem.* **2012**, *51*, 5037−5049.

(13) (a) Jamali, S.; Ghazfar, R.; Lalinde, E.; Jamshidi, Z.; Samouei, H.; Shahsavari, H. R.; Moreno, M. T.; Escudero-Adán, E.; Benet-Buchholz, J.; Milic, D. Cyclometalated Heteronuclear Pt/Ag and Pt/Tl Complexes: a Structural and Photophysical Study. *Dalton Trans.* **2014**, *43*, 1105−1116. (b) Jamali, S.; Mazloomi, Z.; Nabavizadeh, S. M.; Milić, D.; Kia, R.; Rashidi, M. Cyclometalated Cluster Complex with a Butterfly-Shaped Pt_2Ag_2 Core. *Inorg. Chem.* **2010**, *49*, 2721−2726.

(14) Yersin, H. *Highly Efficient OLEDs with Phosphorescent Materials*; Wiley-VCH: New York, 2007.

(15) (a) Chassot, L.; von Zelewsky, A. Cyclometalated Complexes of Platinum(II): Homoleptic Compounds with Aromatic C,N Ligands. *Inorg. Chem.* **1987**, *26*, 2814−2818. (b) Chassot, L.; Muller, E.; von Zelewsky, A. cis -Bis(2-pbenylpyridine)platinum(11) (CBPPP): A Simple Molecular Platinum Compound. *Inorg. Chem.* **1984**, *23*, 4249−4253. (c) Jolliet, P.; Gianini, M.; von Zelewsky, A.; Bernardinelli, G.; Stoeckli-Evans, H. Cyclometalated Complexes of Palladium(II) and Platinum(II): cis-Configured Homoleptic and Heteroleptic Compounds with Aromatic ĈN Ligands. *Inorg. Chem.* **1996**, *35*, 4883−4888. (d) Gianini, M.; Forster, A.; Haag, P.; von Zelewsky, A.; Stoeckli-Evans, H. Square Planar (SP-4) and Octahedral (OC-6) Complexes of Platinum(II) and -(IV) with Predetermined Chirality at the Metal Center. *Inorg. Chem.* **1996**, *35*, 4889−4895. (e) Gianini, M.; von Zelewsky, A.; Stoeckli-Evans, H. Chiral Cyclometalated Platinum(II) and Palladium(II) Complexes with Derivatives of Thienylpyridine as Ligands: Helical Distortion of the Square Planar (SP-4) Geometry. *Inorg. Chem.* **1997**, *36*, 6094−6098.

(16) (a) Abramovitch, R. A.; Saha, J. G. 404. Aromatic substitution. Part III. Reaction of pyridine with ortho-substituted phenyl radicals, and the influence of oxygen upon isomer ratios in the Gomberg-Hey reaction. *J. Chem. Soc.* **1964**, 2175−2187. (b) Kalyani, D.; Dick, A. R.; Anani, W. Q.; Sanford, M. S. Scope and selectivity in palladium-catalyzed directed C-H bond halogenation reactions. *Tetrahedron* **2006**, *62*, 11483−11498. (c) Kim, K.; Jung, Y.; Lee, S.; Kim, M.; Shin, D.; Byun, H.; Cho, S. J.; Song, H.; Kim, H. Directed C−H Activation and Tandem Cross-Coupling Reactions Using Palladium Nanocatalysts with Controlled Oxidation. *Angew. Chem., Int. Ed.* **2017**, *56*, 6952−6956.

(17) Juliá, F.; González-Herrero, P. Aromatic C-H Activation in the Triplet Excited State of Cyclometalated Platinum(II) Complexes Using Visible Light. *J. Am. Chem. Soc.* **2016**, *138*, 5276−5282.

(18) (a) Reinartz, S.; White, P. S.; Brookhart, M.; Templeton, J. L. Syntheses of Platinum(IV) Aryl Dihydride Complexes via Arene C−H Bond Activation. *Organometallics* **2001**, *20*, 1709−1712. (b) Zhang, F.; Kirby, C. W.; Hairsine, D. W.; Jennings, M. C.; Puddephatt, R. J. Activation of C−H Bonds of Arenes: Selectivity and Reactivity in Bis(pyridyl) Platinum(II) Complexes. *J. Am. Chem. Soc.* **2005**, *127*, 14196−14197. (c) Heyduk, A. F.; Driver, T. G.; Labinger, J. A.; Bercaw, J. E. Kinetic and Thermodynamic Preferences in Aryl vs Benzylic C−H Bond Activation with Cationic Pt(II) Complexes. *J. Am. Chem. Soc.* **2004**, *126*, 15034−15035.

(19) Forniés, J.; Giménez, N.; Ibáñez, S.; Lalinde, E.; Martín, A.; Moreno, M. T. An Extended Chain and Trinuclear Complexes Based on Pt(II)-M (M = Tl(I), Pb(II)) Bonds: Contrasting Photophysical Behavior. *Inorg. Chem.* **2015**, *54*, 4351−4363.

(20) Fuertes, S.; Chueca, A. J.; Martín, A.; Sicilia, V. Pt2Tl Building Blocks for Two-Dimensional Extended Solids: Synthesis, Crystal Structures, and Luminescence. *Cryst. Growth Des.* **2017**, *17*, 4336−4346.

(21) Belío, Ú.; Fuertes, S.; Martín, A. Synthesis and Characterization of a "Pt3Tl" Cluster Containing an Unprecedented Trigonal Environment for Thallium(I). *Inorg. Chem.* **2013**, *52*, 5627−5629.

(22) (a) Rubinstein, L. I.; Pignolet, L. H. Kinetic Investigation of Homogeneous H_2-D_2 Equilibration Catalyzed by Pt-Au Cluster Compounds. Characterization of the Cluster $[(H)Pt(AuPPh_3)_9](NO_3)_2$. *Inorg. Chem.* **1996**, *35*, 6755−6762. (b) Hayoun, R.; Zhong, D. K.; Rheingold, A. L.; Doerrer, L. H. Gold(III) and Platinum(II) Polypyridyl Double Salts and a General Metathesis Route to Metallophilic Interactions. *Inorg. Chem.* **2006**, *45*, 6120−6122. (c) Zhang, L.-Y.; Xu, L.-J.; Wang, J.-Y.; Zeng, X.-C.; Chen, Z.-N. Photoluminescence and Electroluminescence of Cationic $PtAu_2$ Heterotrinuclear Complexes with Aromatic Acetylides Metathesis Route to Metallophilic Interactions. *Dalton Trans.* **2017**, *46*, 865−874. (d) Juliá, F.; Jones, P. G.; González-Herrero, P. Synthesis and Photophysical Properties of Cyclometalated Platinum(II) 1,2-Benzenedithiolate Complexes and Heterometallic Derivatives Obtained from the Addition of $[Au(PCy_3)]^+$ Units. *Inorg. Chem.* **2012**, *51*, 5037−5049. (e) Stork, J. R.; Rios, D.; Pham, D.; Bicocca, V.; Olmstead, M. M.; Balch, A. L. Metal−Metal Interactions in Platinum(II)/Gold(I) or Platinum(II)/Silver(I) Salts Containing Planar Cations and Linear Anions. *Inorg. Chem.* **2005**, *44*, 3466−3472. (f) Goto, E.; Begum, R. A.; Ueno, C.; Hosokawa, A.; Yamamoto, C.; Nakamae, K.; Kure, B.; Nakajima, T.; Kajiwara, T.; Tanase, T. Electron-Deficient $Pt_2M_2Pt_2$ Hexanuclear Metal Strings (M = Pt, Pd) Supported by Triphosphine Ligands. *Organometallics* **2014**, *33*, 1893−1904. (g) Yip, H.-K.; Lin, H.-M.; Wang, Y.; Che, C.-M. Luminescent heterobimetallic complexes. Electronic structure and spectroscopy of [MPt(dppm)2(C=CPh)2]PF6(M = Au or Ag) and crystal structure of [AuPt(dppm)2(C=CPh)2]PF6(dppm = Ph2PCH2PPh2). *J. Chem. Soc., Dalton Trans.* **1993**, 2939−2944.

(23) Bauer, J.; Braunschweig, H.; Damme, A.; Radacki, K. Reversible Insertion of Platinum into Coinage Group Metal-Halogen Bonds. *Angew. Chem., Int. Ed.* **2012**, *51*, 10030−10033.

(24) (a) Maestri, M.; Sandrini, D.; Balzani, V.; von Zelewsky, A.; Deuschel-Cornioley, C.; Jolliet, P. Absorption Spectra and Luminescence Properties of Isomeric Platinum (II) and Palladium (II) Complexes containing 1,1?-biphenyldiyl, 2-phenylpyridine, and 2,2?-bijpyridine as ligands. *Helv. Chim. Acta* **1988**, *71*, 1053−1059.

(25) Deuschel-Cornioley, C.; Lüönd, R.; von Zelewsky, A. Cyclometalated Compounds of Platinum(II) with two different C, N-aromatic ligands. *Helv. Chim. Acta* **1989**, *72*, 377−382.

(26) (a) Ai, Y.; Li, Y.; Ma, H.; Su, C.-Y.; Yam, V. W.-W. Cyclometalated Platinum(II) Complexes of 1,3-Bis(1-n-butylpyrazol-3-yl)benzenes: Synthesis, Characterization, Electrochemical, Photophysical, and Gelation Behavior Studies. *Inorg. Chem.* **2016**, *55*, 11920−11929. (b) Chen, Y.; Lu, W.; Che, C.-M. Luminescent Pincer-Type Cyclometalated Platinum(II) Complexes with Auxiliary Isocyanide Ligands: Phase-Transfer Preparation, Solvatomorphism, and Self-Aggregation. *Organometallics* **2013**, *32*, 350−353. (c) Turner, E.; Bakken, N.; Li, J. Cyclometalated platinum complexes with

DOI: 10.1021/acs.organomet.8b00907
Organometallics XXXX, XXX, XXX−XXX

luminescent quantum yields approaching 100%. *Inorg. Chem.* **2013**, *52*, 7344−7351. (d) Vezzu, D. A. K.; Deaton, J. C.; Jones, J. S.; Bartolotti, L.; Harris, C. F.; Marchetti, A. P.; Kondakova, M.; Pike, R. D.; Huo, S. Highly Luminescent Tetradentate Bis-Cyclometalated Platinum Complexes: Design, Synthesis, Structure, Photophysics, and Electroluminescence Application⊥. *Inorg. Chem.* **2010**, *49*, 5107−5119.

(27) (a) Balch, A. L.; Rowley, S. P. Solubilizing the thallium-platinum unit of $Tl_2Pt(CN)_4$. Preparation and use of a new crown ether/phosphine hybrid ligand for linking main-group and transition-metal ions *J. J. Am. Chem. Soc.* **1990**, *112*, 6139−6140. (b) Chen, W.; Liu, F.; Xu, D.; Matsumoto, K.; Kishi, S.; Kato, M. Luminescent Amidate-Bridged One-Dimensional Platinum(II)−Thallium(I) Coordination Polymers Assembled via Metallophilic Attraction. *Inorg. Chem.* **2006**, *45*, 5552−5560. (c) Berenguer, J. R.; Forniés, J.; Gómez, J.; Lalinde, E.; Moreno, M. T. Four Thallium(I) Ions Sandwiched by Two Tetraalkynylplatinate ($[Pt(C{\vdots}CR)_4]^{2-}$) Fragments: Synthesis and Luminescent Behavior of Pt_2Tl_4 Species. *Organometallics* **2001**, *20*, 4847−4851. (d) Weissbart, B.; Balch, A. L.; Tinti, D. S. Temperature and magnetic field effects on the luminescence of thallium(1+) tetracyanoplatinate(1-). *Inorg. Chem.* **1993**, *32*, 2096−2103. (e) Nagle, J. K.; Balch, A. L.; Olmstead, M. M. $Tl_2Pt(CN)_4$: a non-columnar, luminescent form of $Pt(CN)_4^{2-}$ containing platinum-thallium bonds. *J. Am. Chem. Soc.* **1988**, *110*, 319−321.

(28) Hill, G. S.; Irwin, M. J.; Levy, C. J.; Rendina, L. M.; Puddephatt, R. J. Platinum(II) Complexes of Dimethyl Sulfide. *Inorganic Syntheses*; Wiley, 1998; Vol. *32*, p 149.

(29) Brandys, M.-C.; Jennings, M. C.; Puddephatt, R. J. Luminescent gold(I) macrocycles with diphosphine and 4,4′-bipyridyl ligands. *J. Chem. Soc., Dalton Trans.* **2000**, 4601−4606.

(30) Grimme, S.; Antony, J.; Ehrlich, S.; Krieg, H. A consistent and accurate ab initio parametrization of density functional dispersion correction (DFT-D) for the 94 elements H-Pu. *J. Chem. Phys.* **2010**, *132*, 154104.

(31) Clark, R. C.; Reid, J. S. The analytical calculation of absorption in multifaceted crystals. *Acta Crystallogr.* **1995**, *51*, 887−897.

(32) SuperNova Eos S2 System. Empirical Absorption Correction. *CrysAlis-Software Package*; Oxford Diffraction Ltd, 2011.

(33) Dolomanov, O. V.; Bourhis, L. J.; Gildea, R. J.; Howard, J. A. K.; Puschmann, H. OLEX2: a complete structure solution, refinement and analysis program. *J. Appl. Crystallogr.* **2009**, *42*, 339−341.

(34) Agilent. *AutoChem 2.0, in Conjunction with OLEX2*; Agilent Technologies UK Ltd: Yarnton, Oxfordshire, England, 2011.

(35) Sheldrick, G. M. A short history ofSHELX. *Acta Crystallogr.* **2008**, *64*, 112−122.

(36) Spek, A. L. Structure validation in chemical crystallography. *Acta Crystallogr., Sect. D: Biol. Crystallogr.* **2009**, *65*, 148−155.

DOI: 10.1021/acs.organomet.8b00907
Organometallics XXXX, XXX, XXX−XXX